Robustness of Corroded Reinforced Concrete Structures. A structural performance approach.

Eduardo S. Cavaco[a*], Joan R. Casas[b], Luis A. C. Neves[a], Alfredo E. Huespe[c]

[a] *Universidade Nova de Lisboa, Quinta da Torre, 2829-516 Monte de Caparica, Portugal*; [b] *Technical University of Catalunya, Civil Engineering Department, c/Gran Capitan s/n, Modulo C1 08034 Barcelona Spain*; [c] *International Center for Computational Methods in Engineering (CIMEC), Santa Fe, Argentina*

(*v3.3 released May 2009*)

The aim of this work is to provide new contributions in order to define more accurately the structural robustness concept, particularly when applied to corroded reinforced concrete (RC) structures. To fulfill such task, several robustness indicators are analyzed and discussed with special emphasis on structural performance based measures. A new robustness definition and a framework to assess it are then proposed, based on the structural performance lost after damage occurrence. The competence of the proposed methodology is then tested comparing the robustness of two reinforced concrete foot bridges under corrosion. The damage considered is the longitudinal reinforcement corrosion level and load carrying capacity is the structural performance evaluated. In order to analyze corrosion effects, a finite element based on a two step analysis is adopted. In the first step a cross section analysis is performed to capture phenomenons such as expansion of the reinforcement due to the corrosion products accumulation; damage and cracking in the reinforcement surrounding concrete; steel-concrete bond strength degradation; and effective reinforcement area reduction. The results obtained are then used to build a 2D structural model, in order to assess the maximum load carrying capacity of the corroded structure. For each foot bridge, robustness is assessed using the proposed methodology.

Keywords: Robustness; Vulnerability; Damage; Structural Performance; Reliability; Corrosion; Deterioration; Reinforced Concrete (RC)

*Corresponding author. Email: e.cavaco@fct.unl.pt

ISSN: 1573-2479 print/ISSN 1744-8980 online

DOI: 10.1080/1573247YYxxxxxxxx
http://www.informaworld.com

1. Introduction

In the last decade, the lifetime reliability of existing structures under deterioration has been analyzed by several authors, including Frangopol and Curley (1987), Lind (1995), Ghosn and Moses (1998), Baker *et al.* (2008). This is a consequence of the maintenance cost increase, expected in the near future.

This concept is fundamental in a large number of structures, particularly highway bridges, reaching, or approaching, their defined time horizon. According to Costs (2002), the direct costs associated with bridge deterioration in the United States reach 8.3 billions of dollars annually, and it is expected that the indirect costs associated to users can be up to ten times higher.

The deterioration of existing structures, in particular reinforced concrete bridges, is mainly due to reinforcement corrosion. In this context, emphasis has been placed on the analysis of the strength reduction in critical sections, assuming homogeneous corrosion over the entire structure. There are two main drawbacks in this approach: firstly, corrosion in reinforced concrete bridges is rarely homogeneous, and usually significant deterioration occurs in relatively limited areas of the structure, which may coincide with critical sections, or not; secondly, defining the safety of a structure based only on the resistance of the critical cross sections or members disregards the ability to redistribute stresses and sustain additional loads, and neglects the effect of the overall system behavior on the structural safety.

Moreover, the analysis of the structural capability to sustain accidental damage or human errors has been subjected to growing interest, mainly due to the increased fear of terrorist attacks. Indeed, this has been a consequence of the events on September 11 (New York, USA-2001), the partial collapse of Ronan Point building (London, UK-1968) or the collapse of the I-35W Mississippi River bridge (Minneapolis, USA-2007), among others. From the structural collapse view point (Eagar and Musso 2001, Pearson *et al.* 2003, NTSB 2008), the common property shared by all of those scenarios is the occurrence of disproportionate consequences in comparison with the initial cause or damage.

Most modern structural design codes provide detailed prescriptions on how to assess the safety of individual components, related with localized damage. However, these codes are far less specific regarding requirements to prevent the overall system failure, and its consequences. Damage tolerance and robustness are emergent concepts, and definitely, desired properties of structures. Nevertheless, at present time, robustness is not well defined and much controversy still remains on the subject. Widely accepted methods to define the robustness of structures are still under development, in particular under COST[1] Action TU-0601[2] - Robustness of Structures.

Although robustness may seem a more interesting concept when applied to terrorist attack situations and other extreme event, it can also be very useful when applied to the context of more probable exposures, such as design loads and deterioration scenarios, among others. Similar tools to those employed in robustness analysis of structures subjected to extreme events, can be used to study the impact of deterioration on structural safety. In fact, deterioration is usually a localized phenomenon that can have varying impact on the overall system safety, depending on the localization of damage, structural

---

[1]COST - European Cooperation in the field of Scientific and Technical Research.

[2]The main objective of COST Action TU-0601 is to provide the basic framework, methods and strategies necessary to ensure that the level of robustness of structural systems is adequate and sufficient in relation to their function and exposure over their life time and in balance with societal preferences in regard to safety of personnel and safeguarding of environment and economy.

typology, materials used and level of stresses, among others.

In summary, the aim of this work is to present some contributions on the definition of structural robustness and relate it with the analysis of corroded reinforced concrete structures using advanced and innovative methods.

2. Literature Review

2.1 *Background on Structural Robustness Definition*

Several authors have tried to define structural robustness. However, a consensus on this term has not been reached. Even if not definitive definition exists, no doubts remain that member by member safety verification is not enough to ensure safety, and a global property defining the system safety is desirable.

The works of Callaway *et al.* (2000), Agarwal *et al.* (2006), Wisniewski *et al.* (2006), Starossek and Haberland (2008), Baker *et al.* (2008) and Eurocode 1 (CEN 2002) give a wide range of structural robustness definitions. Key concepts are shared by these definitions, which can be summarized by: event, causes, damage, environment, structural performance or function and consequences. Notions such as disproportionate or abnormal consequences are also used by several authors, but in a sense of quantifying the relation between the referred key concepts.

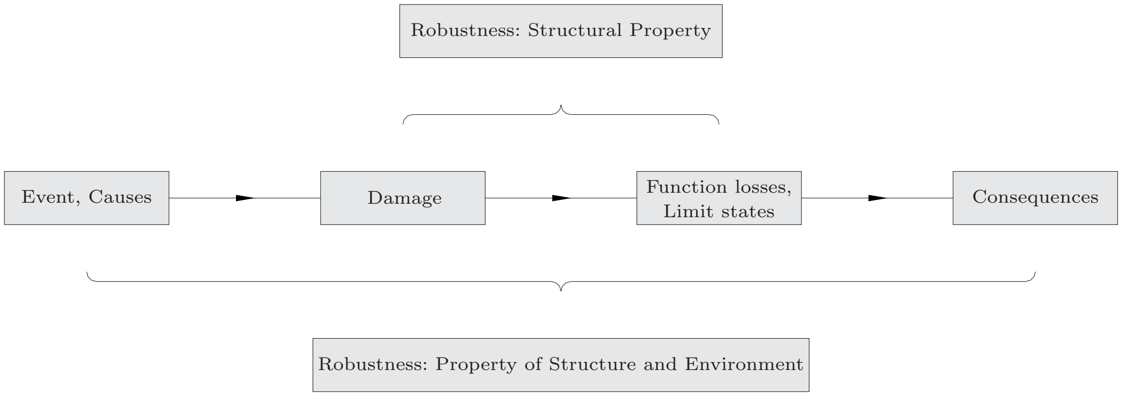

Figure 1. Key Concepts to define robustness.

Figure 1 shows a direct relationship between the key concepts above mentioned, *i.e.*, when a structure is exposed to an event, some damage may occur. This damage may produce a structural performance decrease and consequences may arise from this.

Some authors define robustness as a structural property, independent of the environment where the structure is inserted (Wisniewski *et al.* 2006, Starossek and Haberland 2008). Therefore, in this case, the robustness concept only considers the relation between damage and structural performance decrease.

Alternatively, other authors (Callaway *et al.* 2000, Agarwal *et al.* 2006, Baker *et al.* 2008) and Eurocode 1 (CEN 2002), analyze the environment of the structure and make reference to additional items such as exposure and/or consequences. In this case, robustness is quantified by comparing the trigger event magnitude with the extent of consequences. This means that robustness is defined as a property of both structure and environment, as can be seen in Figure 1.

Thus, depending of the adopted point of view, distinguishing features of the robustness concept can be summarized as follows:

ii) From the first point of view, robustness, considered as a structural property, is related to the structure behavior after damage occurs. This results in a much simpler concept. Its quantification, therefore, can be performed exclusively considering the structural engineering domain;

ii) From the second point of view, robustness, defined as a property of the structure and its environment, is a much wider and complex concept. In fact, when extreme events and indirect consequences of the structural performance loss are considered, robustness assessment becomes an extremely complex task, dependent of several intricate phenomenas, including social and economical environment, among others. Furthermore, a structure that have been considered as robust, may become not robust due to potential changes in the surrounding environment. For instance, if the traffic increases over a bridge, even holding the system safety unchanged, robustness decreases due to increase in the consequences of failure.

2.2 *Background on Robustness Assessment*

In the following, the most important frameworks proposed for several authors to assess robustness, or other related concepts, will be analyzed.

Frangopol and Curley (1987) analyze the effects of damage and redundancy in structural systems, proposing both deterministic and probabilistic measures. In relation with the deterministic approach, the measure of redundancy, R, is defined as the reserve strength between the damage of the components and the system collapse, which can be estimated as follows:

$$R = \frac{L_{Intact}}{L_{Intact} - L_{damaged}} \tag{1}$$

where L_{Intact} is the overall structural collapse load without damage, and $L_{damaged}$ is the overall structural collapse load considering some damage in one, or more, member. The redundancy factor R is equal to 1 when the damaged structure has no reserve strength, and it is infinite when the damage has no influence on the reserve structural strength.

Additionally, in order to take into account the random safety nature, Frangopol and Curley (1987) propose a probabilistic redundancy index β_R defined by:

$$\beta_R = \frac{\beta_{Intact}}{\beta_{Intact} - \beta_{damaged}} \tag{2}$$

where β_{Intact} is the reliability index of the intact system and $\beta_{damaged}$ is the reliability index of the damaged system. The structure is very robust if the probabilistic redundant index is close to infinite. Alternatively, if the probabilistic redundant index assumes values close to 1, it means that robustness tends to be null.

Lind (1995) proposes quantitative measures of system vulnerability and damage tolerance. Vulnerability and damage tolerance are considered, by this author, as complementary concepts. If a system is vulnerable, it is not damage tolerant; and vice versa. The vulnerability V of a system is defined as:

$$V = \frac{P(r_d, S)}{P(r_0, S)} \tag{3}$$

where r_d is the resistance of the damaged system, r_0 is the resistance of the intact system, and S is the loading. $P(r, S)$ is the system failure probability as a function of both loading and resistance effects. The vulnerability V of a system can vary from one when the damage has null impact on the system resistance, to infinite, when it has a huge impact on the system. Alternatively, the damage tolerance T_d of a system is defined, by Lind (1995), as the reciprocal of the vulnerability V:

$$T_d = \frac{P(r_0, S)}{P(r_d, S)} \tag{4}$$

Focusing on highway bridges, Ghosn and Moses (1998) propose an entire methodology to assess, not just the member, but all the system safety. It is considered that a bridge may be considered safe, from the system view point, if:

i) it provides a reasonable safety level against first member failure;
ii) it does not produce large deformations under regular traffic conditions;
iii) it does not reach its ultimate system capacity under extreme loading conditions;
iv) it is able to carry some traffic loads after damage or loss of a main load-carrying member.

Therefore, the following conditions should be checked to insure adequate bridge redundancy and system safety:

1) Member failure limit state: this is the traditional verification of the individual member safety. The corresponding safety level may be represented by the reliability index β_{member}.
2) Serviceability limit state: it is defined as the maximum live load displacement, which is quantified by the value β_{serv}.
3) Ultimate limit state: it is the ultimate bridge system capacity, which is quantified by the value β_{ult}.
4) Damaged condition limit state: it is defined as the ultimate bridge system capacity after the complete removal of one main load carrying component, which is quantified by the value $\beta_{damaged}$.

Following this methodology, the incorporation of the system behavior to the safety assessment is done by the relative reliability indexes $\Delta\beta_i$. They are defined as the difference between the safety indexes of the system and the safety index of the member. In order to guarantee the bridge safety, the obtained relative reliability indexes must be greater than the corresponding target values. And, at the same time, the member safety has to be ensured.

Baker *et al.* (2008) propose a risk-based framework for robustness. Robustness is assessed by computing: *i)* the direct risk R_{Dir}, which is associated with the direct consequences of potential damages to the system, and *ii)* the indirect risk R_{Ind}, which corresponds to the indirect consequences resulting from a failed system. Indirect risk can be interpreted as the risk from disproportionate consequences to the cause of damage, and so, robustness of a system is indicated by the contribution of these indirect risks to the total risk. The robustness index I_{Rob} is then defined as:

$$I_{Rob} = \frac{R_{Dir}}{R_{Dir} + R_{Ind}} \tag{5}$$

and measures the ratio between direct risk and total risk. This index may take values between zero and one. If the system is completely robust, I_{Rob} is equal to one. If all risk is due to indirect consequences, then I_{Rob} is equal to zero. To assess the direct and indirect risks, decision analysis theory and event tree formulation are used. To assess both system direct and indirect risk the consequences associated to each scenario are multiplied by its occurrence probability, and then integrated over all the event space in the event tree.

Biondini and Restelli (2008) present a similar perspective to the one addressed in the current work, *i.e.*, the concept of robustness is used when ordinary events, such as exposure to deterioration, are considered. These authors have studied a trussed structure that was subjected to corrosion of each of its members. Corrosion has been modeled by means of the effective cross section area reduction. In order to assess robustness, several structural performance indicators, considering the undamage state and corrosion levels from 0% to 100%, were compared. For each corrosion level, the deterministic measure for robustness has been defined as:

$$\rho = \frac{f_0}{f_d} \tag{6}$$

where ρ is the robustness index and f_0 and f_d are the structural performance indicators of the undamage and deteriorated states, respectively. The structural performance indicators considered include the stiffness matrix properties, displacements of certain points and pseudo-loads; and damage has been considered as a continuous variable. In this case, a single value for robustness does not exists. Therefore, ambiguous definition for robustness can arise due to the existence of several robustness values for different levels of corrosion and for a given type of damage.

Starossek (2009) study several structural collapse types and propose several robustness measures. Each one is adapted to the type of collapse developed. Some emphasis is put on the *Damaged Based Robustness Measure II*, which is mainly related to the direct consequences produced by an initial damage. It can be computed through:

$$R_{d,int} = 1 - 2\int_0^1 [d(i) - i]di \tag{7}$$

where $R_{d,int}$ is the integral damage-based measure of robustness and $d(i)$ the maximum total damage resulting from, and including, an initial damage of extent i (dimensionless). A value of $R_{d,int}$ equal to one, indicates maximum possible robustness, and a value of zero indicates total lack of robustness.

As can be seen, contrarily to the Biondini and Restelli (2008) proposal, the Starossek (2009) approach considers a single value for robustness.

3. Robustness frameworks analysis

Defining robustness as a property of the structure and its surrounding environment has the handicap of crossing the engineering frontiers. This, makes its quantification much more complex.

According to Canisius *et al.* (2007), most structural failures are due to unexpected loads, design errors, errors during execution, unforeseen deterioration and poor maintenance. These situations can not be prevented by conventional component based code checking formats.

Regarding this scenario, and since there are no risk free structures, actual design codes do not regulate against system failures. Therefore, the main causes of structural collapse can not be predicted and avoided by these codes. The main question is how can this deficiency be overcome. In this case, decision analysis theory and an event tree formulation may be useful to evaluate the situation (see Figure 2).

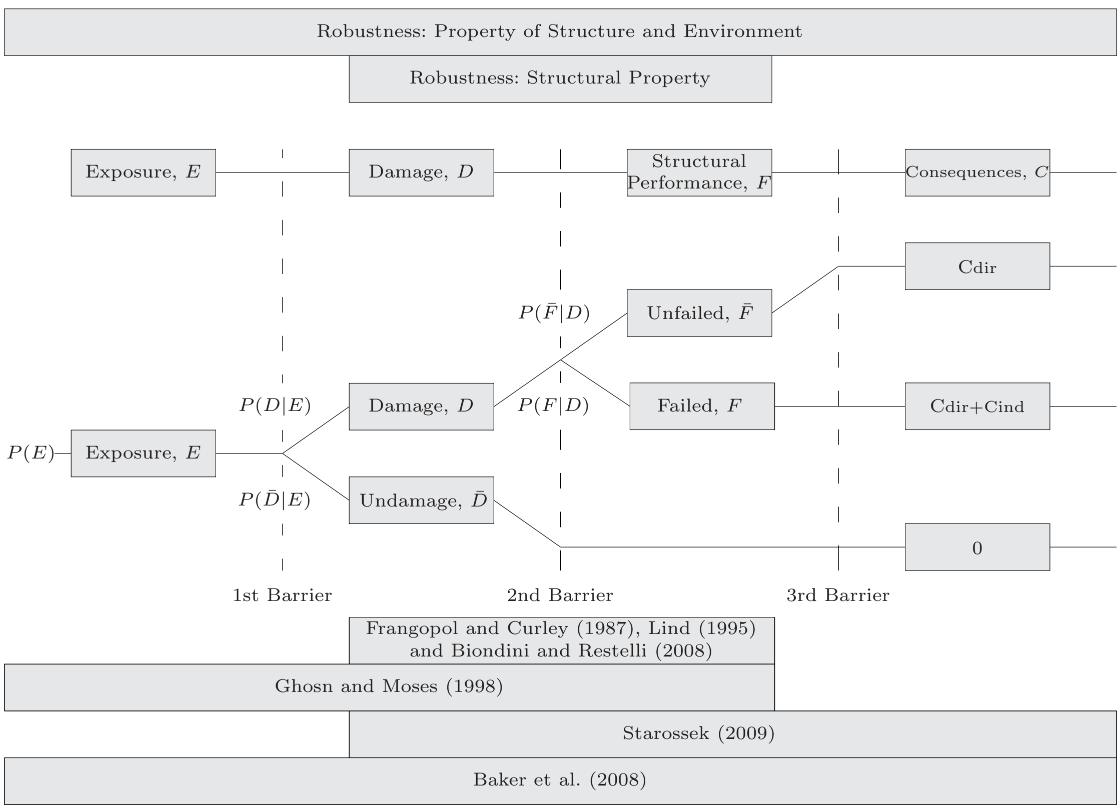

Figure 2. Event Tree.

As presented, the probability of failure can be computed as:

$$P(F) = P(E) \times P(D|E) \times P(F|D) \tag{8}$$

The exposure probability, $P(E)$, is difficult to quantify, especially when extreme events are considered because it depends, not only of the structure itself, but also of its context.

The second term in equation (8), $P(D|E)$, is the probability of damage given a certain exposure. It defines the vulnerability of the structure to a certain exposure, and evaluates the first barrier against failure (see Figure 2). It depends on the design and construction quality control, assessments of loads, design parameters and modeling, among others. Agarwal *et al.* (2006) illustrate this term by considering a wooden house, which is less vulnerable to collapse in an earthquake, but it may be more vulnerable in the event of a fire.

Finally, the third term in equation (8), the probability of failure given a certain damage, $P(F|D)$, evaluates the second barrier against collapse (see Figure 2). It is related with the structural tolerance to damage. This term describes how the structure reacts after a damage occurrence. As it was previously mentioned, codes and norms provides insufficient prescriptions to assess this term.

If robustness is defined as an structural property, the term $P(F|D)$ may be an efficient way of measuring robustness, because it measures the probability of failure given a certain damage. With this in mind, equation (8) may be rewritten in the following qualitative form:

$$Probability\ of\ Failure = Exposure \times Vulnerability \times Robustness \tag{9}$$

In this equation, the failure F has a broader sense, *i.e.*, service or ultimate limit states may be considered, as also, any structural performance decrease. In a similar situation as that presented for damage, the definition proposed by Yao (1985) may be adopted. Following this author, damage refers to any strength deficiency introduced during structure design or construction phase, as well as, any deterioration of strength caused by external loading and/or environmental conditions during the structure lifetime. Thus, a structure can display an initial damage even before it has been exposed to any environmental loadings. In general, damage can exist in the initial structure or be progressively or suddenly imposed upon it.

The event tree presented in Figure 2 and expression (8) can be helpful in understanding the significance of each of the described measures of robustness and rewriting the indicators in terms of partial probabilities:

- Following to Frangopol and Curley (1987), the redundancy index can be rewritten as follows:

$$\beta_R = \frac{\beta_{Intact}}{\beta_{Intact} - \beta_{damaged}} = \frac{\Phi^{-1}(1 - P(F))}{\Phi^{-1}(1 - P(F)) - \Phi^{-1}(1 - P(F|D))} \tag{10}$$

  where Φ is the cumulative normal distribution function.
- From Lind (1995), the damage tolerance index is rewritten as :

$$T_d = \frac{P(r_0, S)}{P(r_d, S)} = \frac{1 - P(F)}{1 - P(F|D)} \tag{11}$$

- From Ghosn and Moses (1998), the target values for the damaged system are reinterpreted as follows:

$$\Delta\beta_{damaged} = \beta_{damaged} - \beta_{member} = \Phi^{-1}(1 - P(F|D)) - \Phi^{-1}(1 - P(D|E)P(E)) \tag{12}$$

  where Φ is the cumulative normal distribution function.
- And from Baker *et al.* (2008), the risk based robustness measure is rewritten as :

$$I_{Rob} = \frac{R_{Dir}}{R_{Dir} + R_{Ind}} = \frac{P(E)P(D|E)P(\bar{F}|D)C_{dir}}{P(E)P(D|E)P(\bar{F}|D)C_{dir} + P(E)P(D|E)P(F|D)C_{ind}} \tag{13}$$

  where C_{dir} and C_{ind} are the direct and indirect consequences respectively.

As can be seen from the above equations, the proposal of Frangopol and Curley (1987) and Lind (1995) are similar. In both cases, robustness increases as the term $P(F|D)$ decreases. From this point of view, and regarding the Figure 2, it can be said that both authors assume robustness as a property of the structure itself.

Robustness, as defined by Biondini and Restelli (2008), is not a probabilistic measure. A robust structure is that for which structural performance cannot be significantly affected by damage. This concept is related to the second barrier, which means that the authors consider robustness as a structural property.

From equation (12), and although Ghosn and Moses (1998) do not account for consequences, robustness is defined as an environment property, because in this case, it takes into account the term $P(E)$ related with the exposure.

Damaged based measure II, proposed by Starossek (2009), measures the relation between the initial damage and the total damage resulting from it. This measure seems to be a structure property if total damage accounts only with total structure damage. However, if total damage takes into account the damage occurred on the structure environment, robustness becomes a property of the structure and its environment.

Finally, as can be seen from the analysis of equation (13) and Figure 2, the risk based robustness index (defined by (Baker *et al.* 2008)) is the most complete approach describing failure. It takes into accounts all the probabilities, from exposure to consequences. Obviously, in this case, robustness is assumed as a structure and environment property.

In order to maximize robustness index, it is possible to create a third barrier, defining whenever some specific procedure has been adopted during design stage. For instance, considering a fire event, the structure can be designed to sustain loads for a long period of time. Thus, it would be possible to rescue occupants, even when the structural collapse eventually happens. This would minimize the failure indirect consequences, increasing the risk based robustness index. To take this into account, a new term in equation (13) may be added in order to minimize indirect risk. This term would be the probability of having certain levels of indirect consequences, given failure occurrence: $P(C_{ind}|F)$.

4. Robustness assessment based on structural performance

Since exposure, at least for design exposures, and the respective component safety are included in design codes, the next step is to assess the system safety, which corresponds to the term $P(F|D)$ in equation (8), and the final step is to quantify the collapse consequences.

Discussion about which approach, risk or performance based designs, is more efficient, is not the objective of this work. In order to assess system safety using both design strategies, it is necessary to understand how structure behaves under damage. In the present work, robustness is assumed to be a structure property. Risk is assumed to be a structure and environment property given by the following qualitative expression :

$$Risk = Exposure \times Vulnerability \times Robustness \times Consequences \tag{14}$$

Therefore, in order to define precisely the robustness concept as widely as possible, it is proposed that robustness is defined by:

Robustness is a structural property which measures the degree of structural performance remaining after damage occurrence. This relation can take many different forms, depending of the limit state (from service to ultimate limit state) that is adopted in the *structural evaluation. Damage definition is taken from Yao (1985), and can vary from a simple degradation state to a more serious damage scenario such as a column or beam failure, among others.*

The concept behind this definition is not to limit, neither the functions spectrum nor the damage scenarios allowing engineers to choose which performance indicator is more suitable for the designing type under study. At the same time this definition allows the consideration of different types of damage scenarios which is an advantage since some structural types are more susceptible to certain types of damage than others. An additional objective of this proposal is to bring the robustness concept into the structural domain allowing quantification as an intermediate step in the process of system safety and risk assessment.

Now that robustness is defined it is necessary to propose a framework to assess it. In order to do perform such a task, some fundamental concepts from previous proposed measures, also defining robustness as a structural property, are used. The proposal of Biondini and Restelli (2008), although deterministic, is found very attractive as it considers damage as a continuous variable, since the structure could behave efficiently for a damage level, while displaying a sudden collapse for a slightly superior damage level. On the other hand, the *damage based measure II*, proposed by Starossek (2009), is very precise. Even considering damage as a continuum variable, it gives a unique robustness value by integrating the overall damage spectrum.

Joining the positive aspects of both proposals, and allowing the generalization for the structural performance indicator and damage scenario as suggested on the proposed definition, a robustness index $I_{R,D}$ can be defined by the area below the curve which corresponds to the normalized structural performance, $f(D)$, function of the normalized damage D:

$$I_{R,D} = \int_{D=0}^{D=1} f(D)dD \qquad (15)$$

Regard that, although the proposed robustness index might seems too simple, in fact its simplicity and/or accuracy depends on the performance indicator used to define $f(D)$. If $f(D)$ is a simple measure, than the proposed index is in fact quite simple. Let's say, for example, that the performance indicator is the structural load carrying capacity, $R(D)$. Consequently $f(D)$ would be obtained through the ratio $R(D = d)/R(D = 0)$ where D is any damage scenario resulting from an exposure. In this case $I_{R,D}$ would represent the average normalized load carrying capacity of the damaged structure. Remark that in this case $I_{R,D}$ would be a generalization of Biondini and Restelli (2008) proposal. On the other hand, if $f(D)$ is based on a more complex performance indicator, the model grows in complexity. If, for example, the reliability index is selected to be the performance indicator, than $I_{R,D}$ is similar to the proposal of Frangopol and Curley (1987) (equation (2)) but considering the overall damage spectrum. However, $I_{R,D}$ is a much more sensitive index since both f and D are normalized. Consequently, robustness index $I_{R,D}$ may vary from 0, if a minimum damage level produces the entire loss of structural performance, to 1, if the damage does not produces influence on the structural performance. In Figure 3, curves (a), (b) and (c) represent, respectively, intermediate increasing robustness. Remember that β_R as proposed on equation (2) may vary from 1 to infinite making this index more insensitive. The performance indicator selected can also be the failure probability and damage can only assume a single value, than $f(D)$ can be defined as the ratio $f(D) = P(F|D = 0)/P(F|D = d)$, becoming the damage

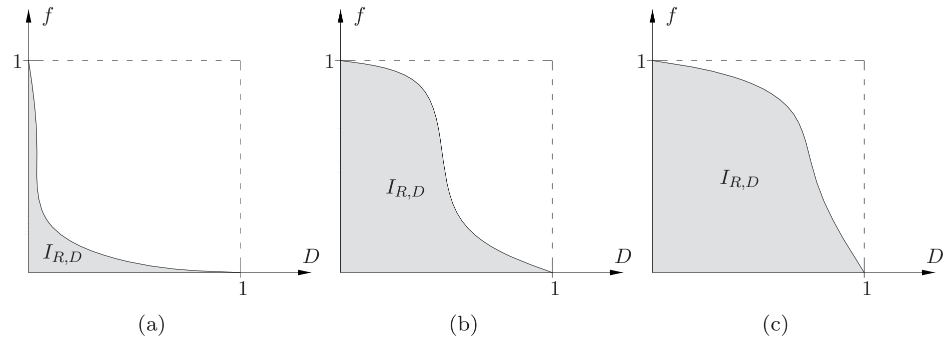

Figure 3. Normalized structural performance f as a function of normalized damage d. (a)Minimum robustness; (b) intermediate robustness; (c) maximum robustness.

tolerance index proposed by Lind (1995).

It might be tempting to compare directly the proposed measure with Ghosn and Moses (1998) or even with Baker *et al.* (2008) proposals. However this is a not possible since these measures are based on different perceptions of robustness. Consequently, it is not possible to define which measure is best, since all proposals have vantages and disadvantages since they are based on different concepts. Despite all, there is no doubts that risk assess is the ultimate goal on decision making. However risk measures require a huge amount of information, in most cases unknown at design stage and outside engineers domain. On the other hand, the proposed measure depends only on structural behavior and it is polyvalent enough to be suitable to use on a broader context of structural types and damage scenarios and by engineers in general.

5. An application example: robustness quantification of a RC structure subjected to corrosion

As expected, the best form to assess robustness would be through the correct quantification of probabilistic performance indicator as the term $P(F|D)$. However in most practical and real situations this represent a difficult task and that is the reason why in the past robustness assess have been done exclusively through educational rather than realistic examples. On the contrary, in this paper a real RC structure subjected to reinforcement corrosion is analyzed. However, and due to increase complexity associated to a probabilistic analysis of such an intricate behavior, a deterministic performance indicator was selected to assess robustness.

In order to reach this objective, the adequate estimation of the corrosion effects on RC structures must be analyzed. This requires the consideration of a number of mechanisms that degrade the structural response including reinforcement net area reduction and reinforcement expansion due to the accumulation of the corrosion products. This last effect leads to damage, cracking and splitting of the concrete reinforcement cover, and also, to degradation of steel-concrete bond. Considering that the steel-concrete adherence plays a fundamental role in the stress transfer mechanism between both components, its degradation could lead to a notable structural load carrying capacity loss. Therefore, its correct prediction becomes one of the most important aspects in this type of structural safety assessment.

5.1 *Methodology of analysis*

The analysis of corrosion effects in RC structures is performed through numerical simulation. A Finite Element (FE) methodology is adopted, which is coupled with an advanced constitutive model for simulating the most important degradation phenomena caused by corrosion. This methodology is taken from **?**, where it was validated through experimental results.

Three fundamental ingredients of the methodology provide a valid framework for the analysis of the typical fracture phenomenon observed in RC structures. This phenomenon eventually determines the structural failure mechanism. They are:

i) **a concrete constitutive relation based on a regularized isotropic continuum damage model**. This model assumes an elastic response (described by the Young-modulus E and Poisson ratio ν) until stress reaches concrete resistance, f_t, for tensile stress (and compressive resistance, f_c, for compressive stress). After that, it is assumed that the degradation of the elastic material properties occurs. This degradation results from the initiation, growth and coalescence of micro cracks, which can be modeled by introducing a scalar internal damage variable d ($d \in [0, 1]$). Figure 4 depicts the corresponding 1D stress-strain response, where it can be observed that the degradation of the elastic stiffness is given by the factor $(1 - d)$. A regularized evolution law, defined through the concrete fracture energy G_f, is provided for $(\dot{d})$, the damage variable derivative. This regularization introduces, in the model, the correct energy dissipation when a propagating crack is simulated. A full detailed description of the model can be found in Oliver (2000).

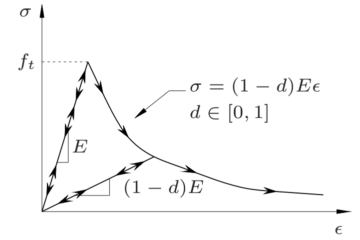

Figure 4. Isotropic Continuum Damage Model.

ii) **a strong discontinuity kinematics based on the continuum strong discontinuity approach,** *CSDA* (Oliver *et al.* 2002). With this kinematics approach, it is possible to model cracks that are characterized as jumps in the displacement field.

According to the *CSDA* methodology, if a body Ω (as shown in Figure 5), experiences a strong discontinuity (*i.e.*, a crack formation) across the surface S described by the normal n, the displacement field will experience a jump. Considering that the surface S divides the solid in two domains Ω^+ and Ω^-, with the vector n pointing toward Ω^+, then the displacement $u(x)$, and the compatible strain field $\epsilon(x)$, can be written in the following form:

$$u(x) = \overbrace{\bar{u}(x)}^{continuous} + \overbrace{H_S(x)[\![u]\!](x)}^{discontinuous} \; ; \; H_S(x) = \begin{cases} 1 \; \forall \; x \in \Omega^+ \\ 0 \; \forall \; x \in \Omega^- \end{cases} \tag{16}$$

$$\epsilon(x) = \nabla^{sym} u(x) = \underbrace{\bar{\epsilon}(x)}_{regular: \nabla^{sym}\bar{u}(x)} + \underbrace{\delta_S(x)\left([\![u]\!] \otimes n\right)^{sym}}_{singular} \tag{17}$$

where $\bar{u}(x)$ is a continuous function, $[\![u]\!](x)$ represents the displacement jump across the discontinuity S and $H_S(x)$ is the Heavisides step function shifted to S. The strain field shows a singular term, the second term in equation (17), given by the Dirac's delta distribution $\delta_S(x)$ which must be regularized in the computational implementation. Additional details about the CSDA and its implementation can be found in Oliver *et al.* (2002).

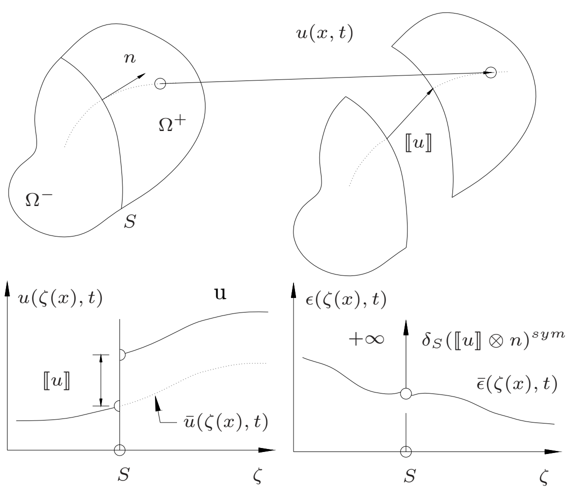

Figure 5. Continuum Strong Discontinuity Approach.

iii) **an embedded strong discontinuity finite element**; additional details about this topics can be found in the work of Oliver *et al.* (2002).

Using these concepts, **?** have developed a two-stage procedure based on 2D FE analysis, which captures the fundamental 3D effects caused by the reinforcement corrosion.

In the first stage, a mesoscopic FE analysis of a generic cross section of the analyzed structural member is carried out. Reinforcements are modeled using a linear elastic constitutive relation which interact with the concrete, through an interface model (contact FE) that imposes unilateral contact and transfers the shear and normal stresses between both materials. The accumulation of the corrosion products is simulated through an equivalent steel bar expansion.

In a second stage, the concrete degradation, evaluated in the first stage, caused by the rebar expansion effect, is averaged (variable d) in different horizontal slices of the member cross section, and transfered, as an equivalent damage map, to a 2D structural bending model, which eventually capture the ultimate load carrying capacity of the structural member. Additional details of this model are presented in subsection 5.2.2.

5.2 *Bridge structural member analysis*

Two small foot bridges are considered in the present study (Cavaco 2009). An identical structural model is chosen for both design solutions. The structural model is composed by a simply supported beam with 14.0m of free span, subjected to a midspan concentrated load, as depicted in Figure 6.

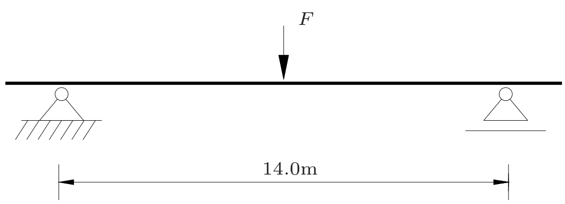

Figure 6. Structural model.

A 2.0m walking path is adopted and the design value for the load carrying capacity is taken from CEB (1993). Two cross sections are designed according to CEB (1993). The first structure is a slab, displayed in Figure 7, and the second one is a I-beam, displayed in Figure 8. In both cases, the transversal reinforcement was over designed because corrosion of this part of reinforcement was neglected. Thus, the expected failure mechanism is a plastic hinge formation at the mid span due to the yielding of the longitudinal reinforcement.

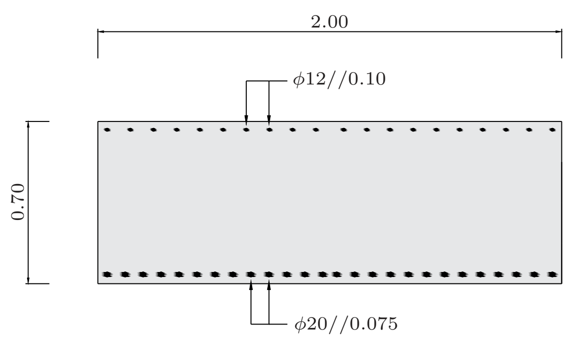

Figure 7. Slab design solution.

Identical material parameters are used for both design solutions. The mechanical properties adopted for concrete are summarized in Table 1, where f_t and f_c are the maximum tension and compressive stresses. E, ν and G_f are the Young's modulus, the Poissons ratio and the fracture energy respectively. Reinforcement is modeled by assuming a perfect

Table 1. Concrete Material Properties

Material	f_t (MPa)	f_c (MPa)	E (GPa)	ν	G_f (kN/m)
Concrete	3.0	30.0	30	0.20	0.10

elastoplastic behavior with a yield stress of 400MPa and Young's modulus of 200GPa.

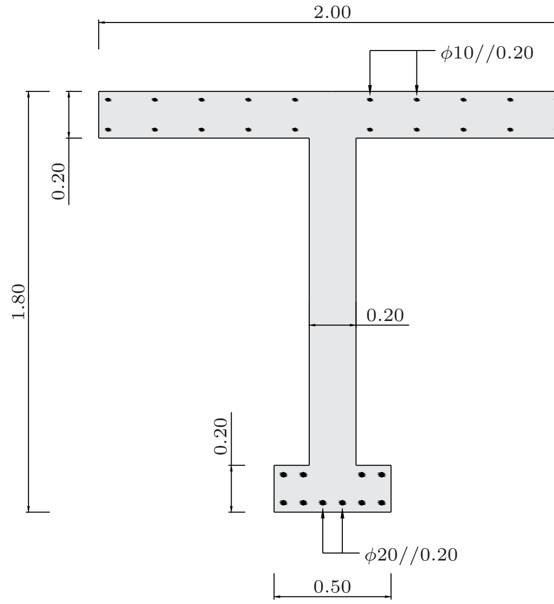

Figure 8. I-beam design solution.

In order to assess robustness, the considered damage corresponds to the corrosion level percentage, X_p, in terms of volume of the longitudinal reinforcement, while the studied structural performance is the load carrying capacity F. Although it would be preferable to select a probabilistic performance indicator since it considers the uncertainties in structural response, the fact is that the considered model is extremely complex and, at the present time, the computational cost of such analysis is too large. Moreover, in most practical situations, structures are designed using semi-probabilistic models. Therefore the consideration of a deterministic model calibrated with partial safety factors would be also of great interest. However discussion about the magnitude of these factors overreach the scope of the present work.

5.2.1 First stage: the Cross Section Analysis

The corrosion product accumulation and expansion effect is simulated by a volumetric dilatancy of the steel bars ϵ^0 (Figure 9). Assuming a plain strain state, the total strains ϵ can be obtained by the sum of the strains due to stresses ϵ^e and that due to the referred volumetric dilatancy ϵ^0 (**?**):

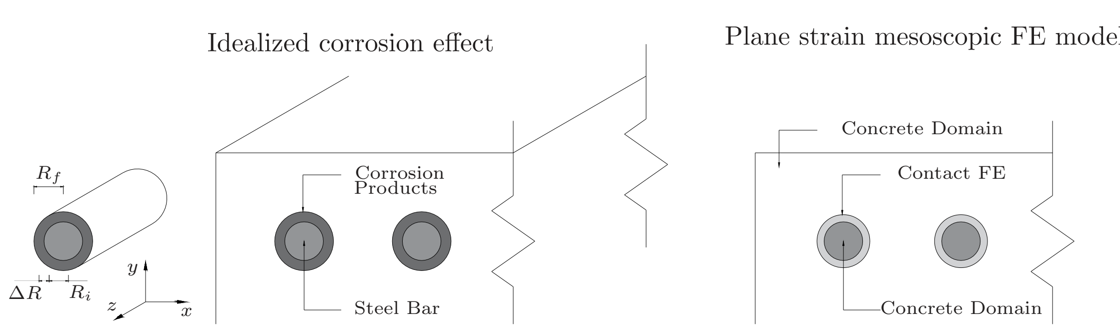

Figure 9. Cross Section Analysis: (a) Idealization of the effect due to the corrosion products; (b) three different domains are spatially discretized in the mesoscopic model.

$$\epsilon = \nabla^{sym} u(x) = \begin{bmatrix} \epsilon_{xx} \\ \epsilon_{yy} \\ \gamma_{xy} \\ \epsilon_{zz} \end{bmatrix} = \begin{bmatrix} \epsilon_{xx} \\ \epsilon_{yy} \\ \gamma_{xy} \\ 0 \end{bmatrix} = \overbrace{\begin{bmatrix} \frac{1}{E}(\sigma_{xx} - \nu\sigma_{yy} - \nu\sigma_{zz}) \\ \frac{1}{E}(\sigma_{yy} - \nu\sigma_{zz} - \nu\sigma_{xx}) \\ 2\frac{1+\nu}{E}\sigma_{xy} \\ \frac{1}{E}(\sigma_{zz} - \nu\sigma_{xx} - \nu\sigma_{yy}) \end{bmatrix}}^{\epsilon^e} + \overbrace{\begin{bmatrix} \mathcal{D} \\ \mathcal{D} \\ 0 \\ 0 \end{bmatrix}}^{\epsilon^0} \tag{18}$$

The variable $\mathcal{D}$ represents the dilational component, which depends on the corrosion attack depth X and can be obtained from the following expression:

$$\mathcal{D} = \frac{R_f^2 - R_i^2}{2R_i^2} \tag{19}$$

where R_i is the initial bar radius and $R_f(X)$ is the final bar radius. Assuming incompressibility of the accumulated corrosion products and taking the bar radius increment equal to the corrosion depth X, the final bar radius can be computed as:

$$R_f = R_i + \Delta R \tag{20}$$

During the cross section analysis, and for a determined corrosion depth X, the dilation $\mathcal{D}$ was applied incrementally during the nt time steps required to perform the non-linear analysis.

Results:

The analysis is performed for corrosion levels, X_p, from 0% to 100%, or for corrosion depths, X, from 0 to R_i. Note that corrosion effect is simulated as a volumetric expansion, therefore, with the corrosion level increase, the concrete around the steel rebars evolves into a tension condition. As a result, and since an isotropic continuum damage model was considered (see Figure 4), concrete around rebars starts losing strength until cracking. As explained previously, the damage variable d is used to characterize the deterioration scenario and when it reaches a value close to one it means that concrete loses all its resistance and a crack may start developing. In Figure 10(a), the damage d concrete map, for the slab design solution and a volumetric expansion equivalent to 50% corrosion level, is presented. As shown, the concrete cover damage, around steel bars, becomes evident. As referred before, the finite elements, used to model the cross section, are enriched with the strong discontinuity kinematics approach, which allows crack modeling as jumps in the field displacement. Therefore, areas of isodisplacement lines concentration indicate that a crack is developing. In Figure 10(b), isodisplacement lines are displayed for the same volumetric expansion equivalent to 50% of corrosion level. On the slab top, it is possible to observe small cracks appearing and propagating from the reinforcements to the concrete top surface. On the slab bottom, and since the steel bars are closer together, a unique horizontal crack develops connecting the bars, and leading to the spalling of the concrete cover.

Figure 11(a) and (b) display the damage and isodisplacement lines, respectively, for the I-beam design solution. Considering the same corrosion level, $X_p = 50\%$, in this case, the role played by cracking is much more important, since deep cracks appear, crossing the section flanges from bottom to upper surfaces, and leading to a more dramatic cross section strength loss. It must be noted however, that the effect of the concrete

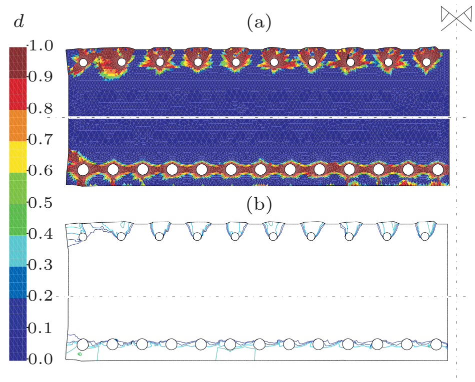

Figure 10. Damage and cracking on slab design solution due to steel bar expansion. (a) Damage d; (b) Isodisplacement lines.

confinement, provided by stirrups, is neglected in the analysis.

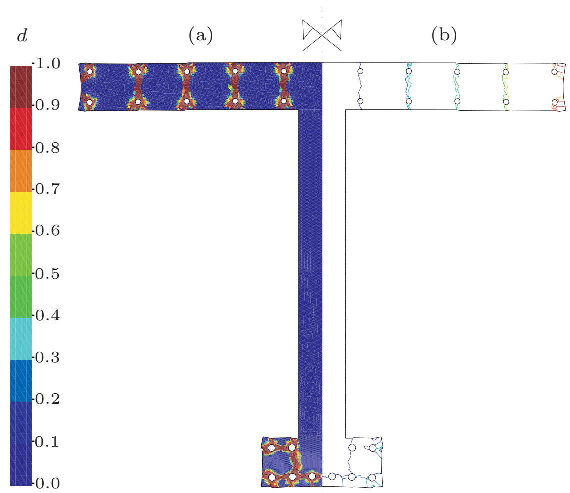

Figure 11. Damage and cracking on I-beam design solution due to steel bar expansion. (a) Damage d; (b) Isodisplacement lines.

5.2.2 Second stage: the 2D longitudinal Analysis of the structural member

In the 2D longitudinal analysis, the reinforced concrete is modeled by means of a homogenized composite material constituted by a matrix, representing the concrete, and long fibers which represent the reinforcements. The homogenized model here adopted is based on the mixture theory proposed by Oliver *et al.* (2008) (see Figure 12). According to the basic hypothesis of this approach, a composite material is a continuum in which each infinitesimal volume is occupied simultaneously by all constituents behaving as a parallel mechanical system. As a consequence, all the constituents are subjected to the same composite strain ϵ, while stresses are given by the weighted sum, in terms of the volume fraction, of the stresses of each constituent.

The concrete is described using an identical approach to that presented in the previous subsection. However, the reinforce effect and the steel-concrete adherence behavior are approached by means of a different and unified mechanical model, which is described in the next subsection.

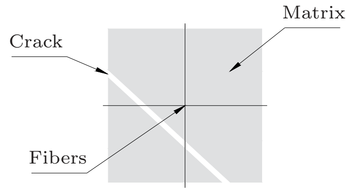

Figure 12. Reinforced concrete as a composite material.

5.2.3 Slipping-fiber model

The reinforcement response is modeled jointly with the concrete-steel interface effect. An unified slipping-fiber series mechanical system, as shown in Figure 13, is adopted. The strain ϵ^f of this system is defined by two additive parts:

$$\epsilon^f = \epsilon^d + \epsilon^i \tag{21}$$

where ϵ^d is the fiber mechanical strain and ϵ^i is an additional strain that should be interpreted as the effect produced by the sliding interface.

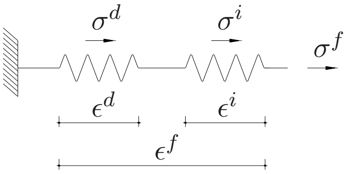

Figure 13. Slipping-fiber model.

The corresponding stress σ^f of the sliding-fiber system, by equilibrium, is identical to the reinforcement stress σ^d and that corresponding to the sliding interface effect, σ^i:

$$\sigma^f = \sigma^d = \sigma^i \tag{22}$$

Both stress-strain relationship (ϵ^i, σ^i and ϵ^d, σ^d) can be computed via a 1D elasto-plastic hardening/softening model. The resulting constitutive behavior for the slipping-fiber system is also a 1D elasto-plastic model with the following characteristics (see Figure 14):

$$\sigma_y^f = min(\sigma_y^d, \sigma_y^i) \tag{23}$$

$$E^f = \frac{1}{\frac{1}{E^d} + \frac{1}{E^i}} \tag{24}$$

in which E^d and σ_y^d are Young's modulus and yield stress steel, respectively, E^i is the interface elastic modulus and σ_y^i is the interface bond limit stress. Considering that, when $E^i \to \infty$ and $\sigma_y^d < \sigma_y^f$, the system provides only the mechanical behavior of the fiber, reproducing a perfect adhesion between concrete and reinforcement bars.

The parameters required to characterize the slipping-fiber model can be obtained from pullout tests. In the present study, under no corrosion, perfect adhesion between steel bars and concrete is considered and a rigid-plastic behavior for the interface is adopted, resulting in $E^i \to \infty$ and $\sigma_y^i = \sigma_y^d$. For a corrosion level, X_p, bond strength degradation

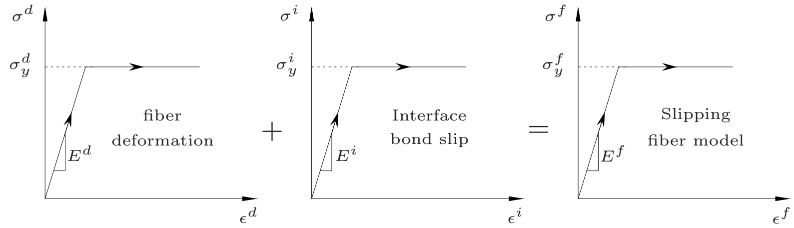

Figure 14. Slipping-fiber model composition.

is considered by assuming $E^i \to \infty$ and $\frac{\sigma^i_y(X_p)}{\sigma^d_y} \leq 1$. This last relation can be predicted through the model presented in the next section.

5.2.4 Bond strength deterioration

Corrosion plays a fundamental role in the bond strength mechanism. Several authors reported a wide range of bond strength values for identical levels of corrosion, see for example Al-Sulaimani *et al.* (1990), Cabrera (1996), Rodriguez *et al.* (1994), Almusallam *et al.* (1996), Amleh and Mirza (1999), Auyeung *et al.* (2000), Lee *et al.* (2002) and Fang *et al.* (2004).

In the present work, the *M-pull* empirical model, developed by Bhargava *et al.* (2007) and based on a large set of different pullout experimental tests, is adopted. It defines the normalized bond strength $\frac{\sigma^i_y(X_p)}{\sigma^i_y(X_p=0)}$ (see Figure 14) as a function of the corrosion level X_p. Corrosion level X_p is the reinforcing bar weight loss expressed as a percentage of original rebar weight. The *M-pull* model can be expressed as:

$$\frac{\sigma^i_y(X_p)}{\sigma^i_y(X_p=0)} = \begin{cases} 1.0 & if \;\; X_p \leq 1.5\% \\ 1.192 \cdot e^{-0.117 X_p} & if \;\; X_p > 1.5\% \end{cases} \tag{25}$$

Notice that experimental data does not take into account the stirrups effect on bond strength deterioration.

5.2.5 Coupling Cross section and 2D longitudinal analysis

Cross section analysis is performed until advanced corrosion depths X are reached. In fact, after the formation of the crack pattern presented in section 5.2.5, there is no need to go further with the analysis because no more cracks will appear.

For each attack depth X, the cross section results are processed as follows. The cross section is divided into horizontal slices and the average value of damage d variable, for each slice, is computed (see Figure 15 (b)). The average damage is then projected on the 2D longitudinal model of the structural member (see Figure 15 (c)).

Particularly, when a deep cracks crosses the complete section of the member, separating one fraction of it from the main member section, it is assumed that this unfastened section takes a damage d equal to 1 (see Figure 15 (a)). Therefore, even in this particular case, the above explained averaging techniques is applied. At the same time, if there are steel bars on these unfastened parts of the section, they are not taken into account in the effective reinforcement area of the longitudinal model.

In the second stage analysis, corresponding to the longitudinal bending model, the corrosion level X_p and the effective reinforcement area for each steel bar are computed, together with the bond strength loss, in order to characterize the slipping-fiber model.

In spite of being an accurate model, some limitations exist, in particular as a result of performing the two steps of the analysis separately. In fact, corrosion effects are

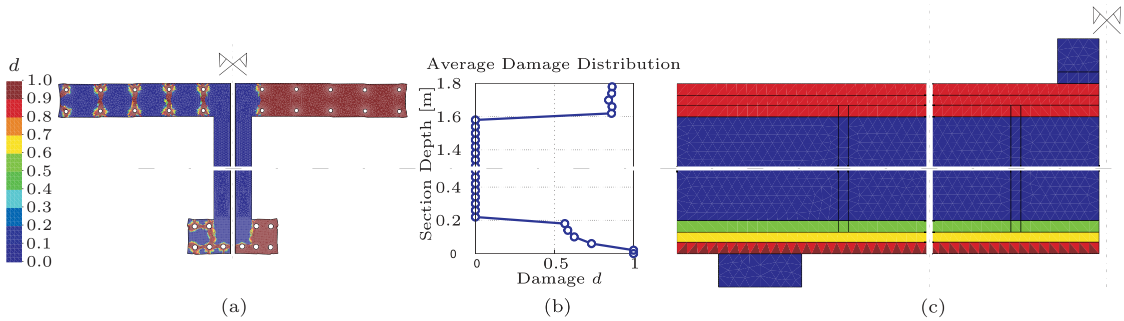

Figure 15. Coupling strategy

considered to act firstly and only after that, is the structure loaded and the carrying capacity calculated. It is certain that both events occur simultaneously and it is known that reinforcement corrosion is aggravated by tension resulting from acting loads. This phenomenon is not considered with the present model in either design solutions.

Results:

Figure 16 shows the load-displacement diagrams corresponding to the slab solution. Each curve represents a given corrosion levels X_p. For the less corroded levels, three stages can be observed in the structural response. A first stage which corresponds to the elastic behavior. This stage ends when the load reaches approximately 400kN. A second stage corresponds to crack spreading and continues until the maximum load is reached. In this stage, it is possible to observe how the structural stiffness is degraded due to cracking. In the third stage, corresponding to the yielding of bottom steel bars, the structure can no longer sustain any load increment. Thus in the third stage the failure mechanism is developed. It consists of a plastic hinge formation just below the load application point.

Comparing the curves for several corrosion levels, it is observed that, as the corrosion level increases, the second stage tends to become shorter. For a corrosion $X_p = 7.7\%$, or higher, the second stage does not exist and after the first crack appears, steel bars immediately reach the yielding stress. When the first crack occurs, stresses are transferred from the concrete to the steel bars. When the steel bars are significantly corroded, and the steel-concrete adherence is deteriorated, rebars cannot support additional stresses, and the structural load carrying capacity falls to lower values.

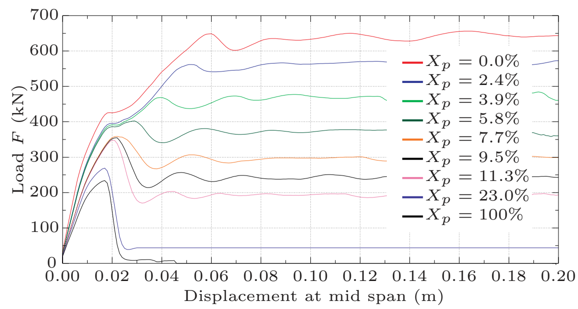

Figure 16. Load-displacement diagram for slab design solution and for several corrosion levels.

Thus, for advanced corrosion states, steel rebars do not play an important role on the ultimate structural load capacity. Their influence increase slightly in the uncraked stage, and are responsible for post–peak load carrying capacity. For a corrosion level of 100%, only concrete contributes to the cross section resistance.

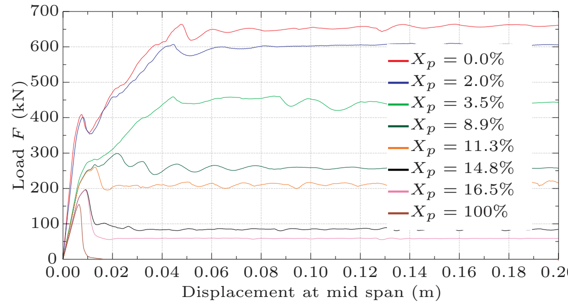

Figure 17. Load-displacement diagram for I-beam design solution and for several corrosion levels.

In Figure 17, similar results are presented for the I-beam design solution. The structural behavior conclusions are quite similar. Nevertheless, in this case, it is possible to observe a larger difference between corroded and uncorroded load carrying capacities. In this case, the peak load decreases from about $650kN$ to $150kN$, for $X_p = 0\%$ and $X_p = 100\%$ respectively. On the slab design case the load reduction is from about $650kN$ to $225kN$ for the same corrosion levels. This means that, without steel bars, the I shape slender cross section is weaker, or, that the influence of steel bars on the overal resistance is higher in the I-beam case.

5.3 *Robustness assessment*

As it has been previously defined, robustness is a property of the structure that measures the degree of structural performance loss due to damage. In this case, structural performance is taken as the peak load, and damage is defined as the corrosion level X_p, which measures the loss of effective reinforcement area.

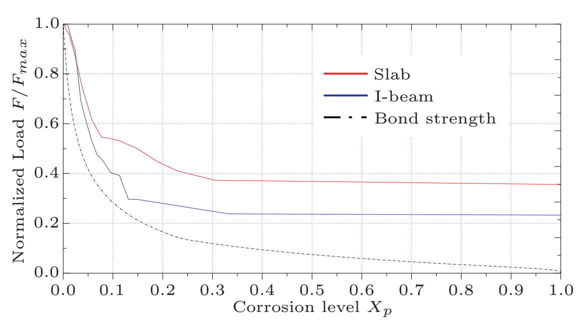

Figure 18. Normalized peak load carrying capacity F/F_{max} and normalized bond strength $\frac{\sigma_y^i(X_p)}{\sigma_y^i(X_p=0)}$ as a function of the corrosion level X_p.

Figure 18 shows the normalized peak load carrying capacity F/F_{max} of the structures versus the corrosion level X_p. In the same figure, the normalized bond strength of the slipping-fiber model versus the corrosion level X_p is also plotted.

From the analysis of Figure 18, it is possible to conclude that bond strength plays a major role for lower corrosion levels. For $X_p \leq 0.075$ and $X_p \leq 0.15$, in the slab and I-beam designs respectively, the bond strength reduction dominates all over other phenomenas causing peak load decrease, such as reinforcement effective area reduction and concrete deterioration.

From Figure 18, it is clear that the I-beam performance curve is more irregular than that observed for the slab curve. The small jumps observed in these curves, are due to cross section cracks occurrence with loss of integrity, as a result of expansion and accumulation of corrosion products. For the slab, the bottom and upper concrete cover spalling occurrence contrasts with the detaching of large parts of both, bottom and upper flanges, in the I-beam case.

For corrosion levels higher than $X_p = 0.075$ and $X_p = 0.15$, in the slab and I-beam designs respectively, both curve slopes tend to zero since the bond strength degradation ratio also decreases, and reinforcement starts losing influence on the overall resistance of the cross section. For $X_p = 0.40$, the bond strength is almost null, and for both cases, concrete is the only material providing structural resistance. As observed for the I-beam design, steel reinforcement has a major influence in the cross section resistance. Thus, the load carrying capacity loss is higher in this case. When steel reinforcement is totally corroded, (*i.e.*, $X_p = 1$), the load carrying capacities are 36% and 23% of the uncorroded state load carrying capacities for the slab and I-beam respectively. The robustness of both solution can be assessed using equation (15):

(1) For the slab design:

$$R = \int_0^1 F/F_{max}(X_p)dX_p = 0.42 \tag{26}$$

(2) For the I-beam design:

$$R = \int_0^1 F/F_{max}(X_p)dX_p = 0.29 \tag{27}$$

As it is expected, robustness results higher for the slab design case.

To confirm the competence of the above measure, and in order to assess the structural robustness, an additional damage variable is considered. It can be observed that bond strength degradation plays an important role on the load carrying capacity. In Figure 19, the normalized load carrying capacity F/F_{max} is plotted against the normalized bond strength degradation $D_{\sigma_y^i}$, given by:

$$D_{\sigma_y^i}(X_p) = 1 - \frac{\sigma_y^i(X_p)}{\sigma_y^i(X_p = 0)} \tag{28}$$

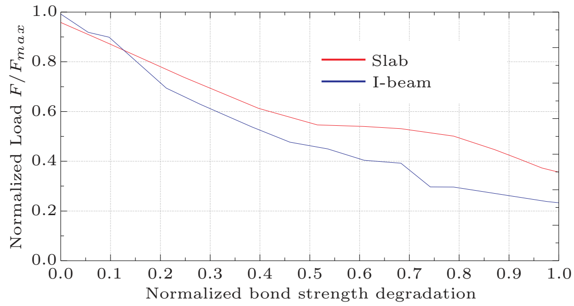

Figure 19. Normalized peak load carrying capacity F/F_{max} as a function of the normalized bond strength deterioration $D_{\sigma_y^i}$.

The structural performance loss (load carrying capacity) displays an almost linear relation with damage (bond strength degradation) for both cases. Applying equation (15):

(1) to the slab design

$$R = \int_0^1 F/F_{max}(D_{\sigma_y^i})dD_{\sigma_y^i} = 0.61 \tag{29}$$

(2) to the I-beam design

$$R = \int_0^1 F/F_{max}(D_{\sigma_y^i})dD_{\sigma_y^i} = 0.51 \tag{30}$$

it can be observed that the slab design results more robust.

If an unreinforced structure had been considered in the present study, robustness would be equal to 1 because corrosion would not affect the load carrying capacity. This is coherent with the adopted definition, i.e., a full robust structure is one that does not loose any performance under damage.

6. Conclusions

Robustness is not a well defined concept and much controversy still remains around the subject. At the same time, corrosion of reinforced concrete structures is an extremely relevant area of research.

In the present work, several robustness definitions and measures are analyzed and discussed. It is concluded that some proposals define robustness as a structural property and others define it as a property of both structure and environment. In this paper, the concept of robustness being a structural property has been adopted and a definition proposed. In order to quantify robustness, a deterministic measure has also been suggested.

To illustrate the proposed robustness index, an example of a corroded reinforced concrete structure has been presented. The example consisted of two simply supported beams with different cross sections, a slab design solution and an I-beam design solution.

The structural performance indicator under analysis is the load carrying capacity and the damage considered is the corrosion level of the bottom reinforcement.

To capture effects of reinforcement corrosion, an advanced finite element methodology has been used, which has been based on the following main features: corrosion was simulated through a steel bar volumetric expansion; an isotropic continuum damage model is used in order to represent concrete behavior; a continuum strong discontinuity approach is adopted to consider concrete cracking; and the mixture theory for the composite material, concrete and reinforcement, is employed.

With the purpose of modeling concrete damage and cracking occurrence due to corrosion products accumulation, an in-plane analysis of the structural member cross section is initially performed. The results of the corroded cross section are then coupled with a longitudinal model of the simply supported beams. And, the structural analysis was finally performed for several corrosion levels. The effect of bond strength deterioration was also considered by means of the *M-pull* model.

Cross section analysis revealed that the reinforcement corrosion produces spalling of concrete cover on the slab design solution. In the I-beam design case, corrosion produces cracks crossing both bottom and upper flanges weakening more significantly the section resistance. This is aggravated by not considering transverse reinforcement confining effect.

Structural longitudinal analysis shows that bond strength deterioration is the major cause of load carrying capacity loss in both beams.

For the two design solutions, normalized load carrying capacity was plotted as a function of corrosion level and as a function of bond strength deterioration. On both cases, the robustness assessment, using the deterministic measure proposed in equation (15), shows that slab solution is more robust. This is mainly due to I-beam cross section integrity loss caused by cracking of bottom and upper flange. An additional reason is the important role played by the steel reinforcement on flexural resistance of I-beam cross section. Consequently reinforcement corrosion has a higher impact on the load carrying capacity of the I-beam.

Vrouwenvelder (1997) Faber and Vrouwenvelder (????) Massey Jr (1951) Olsson *et al.* (2003)

7. Acknowledgments

The authors would like to acknowledge the Research Center in Structures and Construction of Universidade Nova de Lisboa, COST Action TU-0601 and Fundacão para Ciência e Tecnologia, scholarship SFRH/BD/45799/2008, for help supporting this research.

References

Agarwal, J., England, J., and Blockley, D., 2006. Vulnerability analysis of structures. *Structural Engineering International*, 16 (2), 124–128.

Al-Sulaimani, G., Kaleemullah, M., and Basunbul, I., 1990. Influence of corrosion and cracking on bond behavior and strength of reinforced concrete members. *ACI Structural Journal*, 87 (2).

Almusallam, A., Al-Gahtani, A., and Aziz, A., 1996. Effect of reinforcement corrosion on bond strength. *Construction and Building Materials*, 10 (2), 123–129.

Amleh, L. and Mirza, S., 1999. Corrosion influence on bond between steel and concrete. *ACI Structural Journal*, 96 (3), 415–423.

Auyeung, Y., Balaguru, P., and Chung, L., 2000. Bond behavior of corroded reinforcement bars. *ACI Materials Journal*, 97 (2), 214–220.

Baker, J., Schubert, M., and Faber, M., 2008. On the assessment of robustness. *Structural Safety*, 30 (3), 253–267.

Bhargava, K., *et al.*, 2007. Corrosion-induced bond strength degradation in reinforced concrete-analytical and empirical models. *Nuclear Engineering and Design*, 237 (11), 1140–1157.

Biondini, F. and Restelli, S., 2008. Damage propagation and structural robustness. *In*: *Life-Cycle Civil Engineering: Proceedings of the International Symposium on Life-Cycle Civil Engineering, IALCCE'08, Varenna, Lake Como*, p. 131.

Cabrera, J., 1996. Deterioration of concrete due to reinforcement steel corrosion. *Cement & Concrete Composites*, 18 (1), 47–59.

Callaway, D., *et al.*, 2000. Network robustness and fragility: Percolation on random graphs. *Physical Review Letters*, 85 (25), 5468–5471.

Canisius, T., Sørensen, J., and Baker, J., 2007. Robustness of structural systems–a new focus for the joint committee on structural safety (JCSS). *In*: *Proc., 10th Int. Conf. on Application of Statistic and Probability in Civil Engineering (ICASP10).*

Cavaco, E.S., Robustness of Corroded Reinforced Concrete Structures. , 2009. , Technical report, Short Term Scientific Mission, Cost Action TU-0601, Barcelona.

CEB, 1993. Model Code 1990. *Bulletin d'Information nº213/214, Thomas Telford, London.*

CEN, 2002. Eurocode 1: Actions on structures; Part 2: EN 1991-2 Traffic loads on bridges. *Brussels (Belgium):Comite European de Normalization 250.*

Costs, C., Preventive Strategies in the United States. , 2002. , Technical report, FHWA-RD-01-156, Federal Highway Administration, Washington DC.

Eagar, T. and Musso, C., 2001. Why did the World Trade Center collapse? Science, engineering, and speculation. *JOM Journal of the Minerals, Metals and Materials Society*, 53 (12), 8–11.

Faber, M. and Vrouwenvelder, A., Probabilistic model code. , ????. , Technical report, Technical report, Joint Committee on Structural Safety, 2000.

Fang, C., *et al.*, 2004. Corrosion influence on bond in reinforced concrete. *Cement and concrete research*, 34 (11), 2159–2167.

Frangopol, D.M. and Curley, J.P., 1987. Effects of damage and redundancy on structural reliability. *Journal of Structural Engineering*, 113 (7), 1533–1549.

Ghosn, M. and Moses, F., 1998. NCHRP Report 406: Redundancy in Highway Bridge Superstructures. *Transportation Research Board, National Research Council, Washington, DC.*

Lee, H., Noguchi, T., and Tomosawa, F., 2002. Evaluation of the bond properties between concrete and reinforcement as a function of the degree of reinforcement corrosion. *Cement and Concrete research*, 32 (8), 1313–1318.

Lind, N., 1995. A measure of vulnerability and damage tolerance. *Reliability engineering & systems safety*, 48 (1), 1–6.

Massey Jr, F., 1951. The Kolmogorov-Smirnov test for goodness of fit. *Journal of the American Statistical Association*, 46 (253), 68–78.

NTSB, Collapse of I-35W Highway Bridge. Highway Accident Report NTSB/HAR-08/03. , 2008. , Technical report, National Transportation Safety Board.

Oliver, J., 2000. On the discrete constitutive models induced by strong discontinuity kinematics and continuum constitutive equations. *International Journal of Solids and Structures*, 37 (48-50), 7207 – 7229.

Oliver, J., *et al.*, 2002. From continuum mechanics to fracture mechanics: the strong discontinuity approach. *Engineering Fracture Mechanics*, 69 (2), 113–136.

Oliver, J., *et al.*, 2008. Two-dimensional modeling of material failure in reinforced concrete by means of a continuum strong discontinuity approach. *Computer Methods in Applied Mechanics and Engineering*, 197 (5), 332–348.

Olsson, A., Sandberg, G., and Dahlblom, O., 2003. On Latin hypercube sampling for structural reliability analysis. *Structural Safety*, 25 (1), 47–68.

Pearson, C., Delatte, N., *et al.*, 2003. Lessons the Progressive Collapse of the Roman Point Apartment Tower. *Forensic Engineering*, 190–200.

Rodriguez, J., Ortega, L., and Casal, J., 1994. Corrosion of reinforcing bars and service life of R/C Structures: corrosion and bond deterioration. *In*: *Concrete across Borders, Proceedings, Odense, Denmark*, Vol. II.

Starossek, U., 2009. Collapse types and robustness measures. *In*: *COST Action TU0601 Robustness of Structures*, March 2., Coimbra, Portugal.

Starossek, U. and Haberland, M., 2008. Measures of Structural Robustness - Requirements and Applications. *In*: *Proceedings, ASCE SEI 2008 Structures Congress, Crossing Borders*, April 24-26., Vancouver, Canada.

Vrouwenvelder, T., 1997. The JCSS probabilistic model code. *Structural Safety*, 19 (3), 245–251.

Wisniewski, D., Casas, J., and Ghosn, M., 2006. Load capacity evaluation of existing railway bridges based on robustness quantification. *Structural Engineering International*, 16 (2), 161–166.

Yao, J., 1985. *Safety and reliability of existing structures*. Boston: Pitman Publishing.